

Fast Method to Design Air Filtration Solution at Low Energy Cost in Subterranean Train Stations

Pierre-Emmanuel PRETOT¹, Christoph SCHULZ², David CHALET¹, Jérôme MIGAUD³, Mateusz BOGDAN⁴

¹LHEEA lab. (ECN/CNRS)/Centrale Nantes
1 Rue de la Noë, Nantes, France

Pierre-emmanuel.pretot@ec-nantes.fr; David.chalet@ec-nantes.fr

²MANN+HUMMEL GmbH
Schwieberdinger Str. 126, Ludwigsburg, Germany
Christoph.Schulz@mann-hummel.com

³MANN+HUMMEL France
ZA Autoroutière Boulevard de la Communication, Laval, France

Jerome.migaud@mann-hummel.com

⁴AREP L'hypercube
16 av. d'Ivry 75647 Paris Cedex 13
Mateusz.BOGDAN@arep.fr

Abstract – The World Health Organization defines microscopic Particulate Matter (PM) as one of the main air pollutants in terms of exposure to human health risk. According to the European Environment Agency, 10% of European city dwellers were exposed to PM₁₀ concentrations (diameter equal or below 10 µm) above EU standards in 2019. Subterranean train stations are places with high concentrations of fine and ultrafine particulate matter (PM) caused mainly by train activities. However, no specific legislation for subterranean train stations is yet available, and studies on PM concentrations reduction to reduce health risks are currently under investigation. Filtration system solutions are already available to treat these PM and protect travellers and workers. However, energy consumption, maintenance cost/interval, design and operating/control of these systems are crucial factors that must be evaluated via simulation to offer the optimal solution. The optimization method requires a fast and adaptable resolution to assess quickly each situation. From there, a zonal model consisting of an ordinary differential equation giving the evolution of PM concentrations is modified and discretized following the main direction of the stations allowing to precisely place filtration systems along the station within the model. From PM concentrations, air velocity, and train traffic data, physical parameters for the PM model (resuspension, deposition, ventilation and generation) are identified to compute the daily PM concentrations' evolution. For now, PM₁₀ and PM_{2.5} (below 2.5µm) are modelled as they are often monitored. The characterization of the filtration products in terms of filtration efficiency and range is made with 3D CFD (Computational Fluid Dynamics) simulations. This efficiency is modelled in 1D to be added in the PM concentration evolution model. Unlike empirical testing, this simulation approach allows for flexible optimization of local and global filtration solution efficiency with multiple parameters changes, including adjustments to filtration media efficiency and suction volumetric flowrate.

Keywords: Pollution, Particles, Health, Filtration, Energy consumption, Simulation

1. Introduction

World Health Organization has recently stated that air pollution is the most important threat to human health. Based on worldwide studies, the organization has defined air quality guideline (AQG) levels [1] for the main key harmful substances: ozone, nitrogen dioxide, sulfur dioxide, carbon monoxide, particulate matter (PM), etc. These AQG levels are often exceeded in or near cities and mainly due to human activities. This has been highlighted during COVID-19 lockdowns in different cities with important air pollutants concentrations reductions [2]. Transport is an important source of pollution in urban areas. Even if railway public transportation tends to enhance global cities' air quality by reducing in particular the number of vehicles [3], users are subjects to particular air pollution in the case of subterranean facilities.

A complete report from ANSES [4] (Agence nationale de sécurité sanitaire de l'alimentation, de l'environnement et du travail) gives state of knowledge concerning air pollution in railway enclosures. It is concluded that the main pollutants are particulate matters (PM) with high concentrations of coarse ($PM_{10-2.5}$: aerodynamic diameter between 10 and $2.5\mu\text{m}$), fine ($PM_{2.5}$: below $2.5\mu\text{m}$) and ultrafine ($PM_{0.1}$: below $0.1\mu\text{m}$) particles. These particles are primarily metal elements and generated by railway activity [5]. Mainly they are caused by wear e.g. from the braking system, wheel/rail and pantograph/catenary contacts [6].

In order to enhance air quality in railway enclosures in an optimal way, it is first important to have an accurate particle behaviour model. A model developed by Walther *et al* [7] consisting of an ordinary differential equation giving the particle concentration evolution for a particle size class is used as base. 3D computational fluid dynamics was not considered due to simulation duration targeted (a day at minimum) and complexity concerning resuspension phenomena modelling [8] and train traffic or piston effect.

The aim of this study is to propose a complete method for optimization of filtration solutions for subterranean train stations based on a system approach and a multizone particle concentration prediction model considering filtration efficiency, number and placement of devices, flow management and energy consumption, maintenance cost and recurrence, amongst others.

2. Experimental Data

The study case is a subterranean train station from RER near Paris. It is approximately 250m long and 17m large, with two platforms and two central tracks. Only natural ventilation is available (four ventilation shafts with fans available only for fire safety). There are four passenger's accesses and tunnels on both sides of the station.

The train traffic in the station can in general be categorized by two situations. A train can either stop in the station or just pass through. Real train frequencies have been used and can be seen on Figure 3. A specific campaign was launch on 11th and 12th of April 2019 to obtain information on the airflow inside the station. The objective was to better understand the PM concentrations mechanisms. Characterization of airflows inside the station was realized along the platforms on different points and near passenger's accesses. Three three-axis GILL WINDMASTER anemometers installed at different heights were used for sensitivity analysis. Ambient airflows and airflows generated by trains were measured showing mainly important airflow velocities (up to 5m/s) with instantaneous direction changes during train passage (when head and tail of the train reach the measurement position). This campaign also allowed to determine the train velocities. Indeed, a camera was placed perpendicular to the train direction. Knowing the train length, train velocities were recalculated.

Hourly PM_{10} and $PM_{2.5}$ concentrations from the two nearest PM measuring stations from Airparif website were collected (3.75km and 7km distance in opposite direction from the station). Indeed, Airparif is an association commissioned by the French government to monitor air quality of Ile-de-France region (open access to data).

A TEOM 1405-D device (Tapered Element Oscillating Microbalance) is installed in the middle of the station for continuous PM monitoring. With this type of instrument, ambient air is sampled and passes through a filter at a constant flow rate. The filter is continuously weighted and near real-time mass concentrations of particulate matter are calculated. Sampling is here realized at 2.2m above the platform floor for PM_{10} and $PM_{2.5}$. PM concentrations datasets from September 2019 to July 2021 are available (dimensionless 15min median daily values from January to March 2020 on figure 3). A specific PM campaign measurement realized with Palas Fidas Frog (particles numbers and concentrations measurements via optical detection, range: $0.18-100\mu\text{m}$) in the station has highlighted important PM concentration peaks during train passage events (up to $150\mu\text{g}/\text{m}^3$ increase on the platform for PM_{10} in two minutes). Calibration of the device was for outdoor dust and comparison with TEOM shows differences in terms of mean concentrations, but results allow a better understanding of dynamic PM concentrations evolution due to trains (Figure 4).

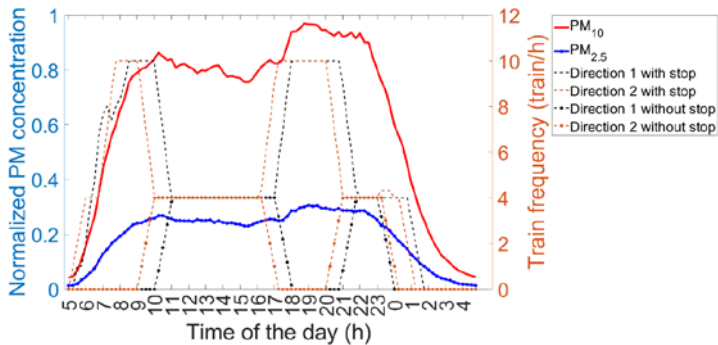


Fig. 3: Normalized median PM_{10} and $PM_{2.5}$ concentrations and train traffic during weekdays (dashed curves)

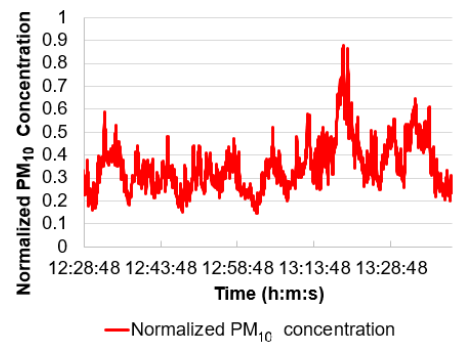


Fig. 4: Normalized PM_{10} concentration from Palas Fidas Frog near TEOM

From November 2020 to March 2021, a filtration solution composed of eight filtration devices was installed and tested inside the station. Five devices were on the TEOM platform and three on the other one at a TEOM distance between 3 and 23m. The driving pollution factor for filter media efficiency selection in the station was PM_{10} . A comparison on the period from January to March between the year 2020 (without lockout period due to COVID-19) without any filtration and 2021 with filtration solution running is available. Impact of COVID-19 on daily passenger numbers and on potential train traffic modifications is unknown. Only period from January to March is used to avoid seasonal changes. Other testing sequences using filtration during two subsequent weeks and then switching off have shown same values for efficiency.

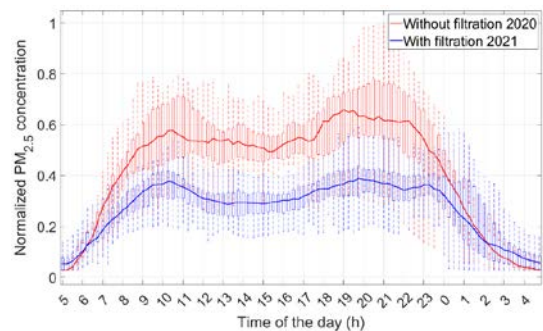
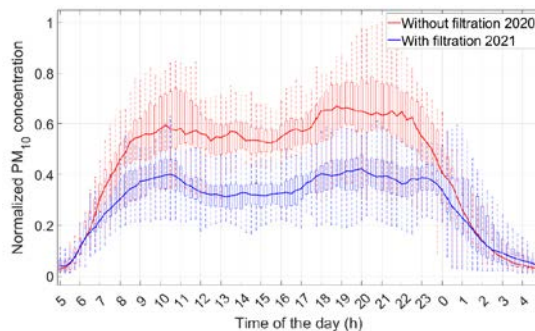


Fig. 5: Normalized median PM_{10} and $PM_{2.5}$ concentrations comparison between period with and without filtration (with statistics: boxes indicate the 25th and 75th percentiles and whiskers most extreme data points not considered outliers)

Efficiency measured on median data is of around 34% for PM_{10} and 36% for $PM_{2.5}$. However, the influence of outdoor PM concentration and airflows are unknown and these efficiency levels are only used as indicators of performance. Mean captured particle mass per day per filtration device has been evaluated during this test campaign by filter weighing before and after use. Finally, a PM mass of 7g/day/device in average has been determined (and 10g/day at maximum for one of these devices). From literature, the maximum PM grain size for train station is around $30\mu m$ and often below $10\mu m$ depending on braking system [6]. Mass captured will then be used as input for model validation.

3. Physical Multi-Zone Model

3.1. Model description

Our physical model is inspired by Walther and Bogdan model. In this one, an ordinary differential equation (ODE) is used to describe the evolution of particulate matter concentration of a given class of particles ($PM_{10-2.5}$ or $PM_{2.5}$). Indeed, PM size have an impact on the dynamic of PM concentration evolution. The evolution of the concentration is defined as the sum of an apparent emission term, a ventilation term and a deposition term (with t in hour):

$$\frac{dC(t)}{dt} = \alpha_a \cdot N^2(t) + \tau(t) \cdot (C_{\text{ext}}(t) - C(t)) - \delta_a \cdot C(t) \quad (1)$$

In this equation, $C(\mu\text{g}/\text{m}^3)$ is the PM concentration inside the station, $C_{\text{ext}}(\mu\text{g}/\text{m}^3)$ is the outdoor PM concentration N is the train traffic frequency (number of trains/hour). Three terms are used: $\alpha_a(\mu\text{g}/\text{m}^3)$ for the apparent emission rate (emission from trains and resuspension of deposited particles), $\delta_a(t)$ for the overall deposition rate and $\tau(t)(1/\text{h})$ for apparent air change rate. This apparent air change rate depends on air change rate from natural and mechanical ventilation τ_0 and air change rate generated by trains and is given by equation 2. The dimensionless coefficient β is defined as the ratio of outdoor air introduced by train by the air station volume.

$$\tau(t) = \tau_0 + \beta \cdot N(t) \quad (2)$$

As the objective of this study is the optimization of filtration solutions, the transition from 0D to 1D is needed to obtain a multi-zone model. Indeed, for each study case, how much and where to place filtration solutions along platforms is of prime importance. Evaluation is realized at each second now (Time $T(\text{s})$). Information on air and train velocities and trains schedules allowed to replace train frequency by precise train passage events. Previous apparent emission term was split into a term for the emission from train and one for the resuspension of deposited particles. This leads to the necessity of a second ODE giving the concentration of deposited particles in the station. Finally, the set of equations giving the evolution of the concentration of particles for a given class and for each zone is:

$$V \cdot \frac{dC(T, x)}{dT} = \alpha \cdot V_t^2(T, x) \cdot L + \frac{\omega}{L} \cdot S \cdot V_{\text{air}}(T, x) \cdot C_{\text{dep}}(T, x) - (v_t + v_n) \cdot \frac{V}{L} \cdot V_{\text{air}}(T, x) \cdot (C(T, x) - C_{\text{ext}}(T, x)) - \delta \cdot V \cdot C(T, x) \quad (3)$$

$$S \cdot \frac{dC_{\text{dep}}(T, x)}{dT} = \delta \cdot V \cdot C(T, x) - \frac{\omega}{L} \cdot S \cdot V_{\text{air}}(T, x) \cdot C_{\text{dep}}(T, x) \quad (4)$$

In these equations: L and V are respectively the length (in m) and the volume (in m^3) of one zone of the model, S is the surface where deposition occurs, V_t and V_{air} are respectively the train and air velocities (m/s). $C_{\text{dep}}(\mu\text{g}/\text{m}^2)$ is the PM concentration deposited on station surfaces. $\alpha(\mu\text{g} \cdot \text{s}/\text{m}^3)$ is the PM emission rate. ω characterizes the level of resuspension per second depending on train velocity and concentration of deposited PM. v_t and v_n characterize respectively the PM transport due to the mean airflow along the train track direction (flow due to trains and natural airflow, $\beta=1$ or $\tau_0=1$ meaning particles attached to the mean airflow). δ is still overall deposition rate but now per second. Arrigoni [9] studied particle emissions from train braking systems. The conclusions were that emission intensities are directly linked to initial train velocity and braking force. Braking force is related to kinetic energy to be dissipated and braking distance. Kinetic energy is given by half the product between the train mass and the square of the train velocity leading to the use of V_t^2 in equation 3.

Henry [8] in its review from 2018 concerning particles resuspension from complex surface concluded that there was no general model taking into account all the aspects of particle resuspension. Indeed, adhesion forces of a particle have to be balanced for particle detachment by aerodynamic forces, vibration or impact with other particle. Particle size and shape and surface roughness are of prime importance here [10]. Study of multi-layers particle system is even more complex. Particle resuspension can be obtained by direct detachment or by rolling or sliding in the first instance and is often given as a function of shear velocity and linked with mean airflow. Due to the large panel of materials with different roughness inside a station and the particular shapes of particles evaluated [5], resuspension in our model needed to be simplified. A mean resuspension level is given depending on airflow velocity and concentration of deposited particles.

Particle deposition is also a complex phenomenon. The deposition level depends mainly on the particle diameter and density, surface orientation, friction velocity (Lai *et al* [11]) and relative humidity [12]. Several physical phenomena

can affect particle transport and deposition velocity: Brownian and turbulent diffusion, gravity, thermophoresis, electrophoresis, amongst others. Brownian diffusion for ultrafine particles and gravitational settling for coarse particles are the predominant mechanisms. In the case of an underground train station, all surface orientations can be encountered.

3.2. Optimization of the model for a configuration with different types of train (with and without stops)

Considering the different traffic situations emission coefficients are split. For all trains contact emissions are considered using α_2 . Trains stopping at the station will in addition create emissions from braking which are covered by α_1 .

Knowing cruising train velocity and deceleration level, velocity profiles are defined. Resuspension and deposition terms are also split into two terms, one during train passages where airflows are highly turbulent and one during natural ventilation.

3.3. Method used for parameter identification

Parameters identification is realized via *lsqcurvefit* function available in Matlab software [13]. This function allows to solve nonlinear curve-fitting problems (data fitting) using least-squares method. By default, it uses the Levenberg-Marquardt algorithm. Bounds are imposed for parameters identification based on physics and literature.

3.4. Filtration term

In order to rate filtration solutions, a filtration term equal to the clean air delivery rate (CADR) is used and given in equation (5). CADR describes the clean air a device delivers per hour to the ambient air and is mainly defined by the volume flow of the device created by the fan (\dot{V}_{Fan}) and the efficiency for the particle size under investigation (η_{media}). If efficiency is increased at constant volume flow also CADR is increased. Looking at real applications an increase of efficiency results in larger pressure drop, higher energy demand of the fan driving the air flow and most likely less volume flow.

$$\text{CADR} = \eta_{\text{media}} \cdot \dot{V}_{\text{Fan}} \quad (5)$$

The filtration term (F) will in consequence represent the apparent filtration efficiency of a filtration device installed in one section of the studied station. The discretization length of the station is adaptable within the model in such a way that a filtration efficiency defined from a 3D CFD simulation for a given volume can be integrated (filtration efficiency depending on aspiration flow, boundary conditions, filter media efficiency, etc.). For example, the conclusion from filtration device testing in 3D CFD on a platform is that it has a range of minimum 10m under the given boundary conditions. Then, discretization length is adapted and polluted air entering the volume would be treated in the 1D model as it would have been done in the 3D CFD. In the 1D model the correlation to 3D CFD is given using a coefficient ε allowing to take into account 3D effects like recirculation zones for example and PM concentration variations inside a volume compared to mean PM concentration encountered into the 1D model. Finally, the filtration term giving the particle mass captured by the filtration device inside a discretized station volume has the following form:

$$F(T, x) = \varepsilon \cdot \text{CADR}(T) \cdot C(T, x) = \varepsilon \cdot \eta_{\text{media}} \cdot \dot{V}_{\text{Fan}}(T) \cdot C(T, x) \quad (6)$$

4. Results and Discussion

In the first part of this section, results for parameter identifications for $\text{PM}_{10-2.5}$ and $\text{PM}_{2.5}$ are given and discussed. In the second part, results from simulations of the real filtration case for the two class of particles using identified parameters are presented and discussed.

4.1. Model parameter identification

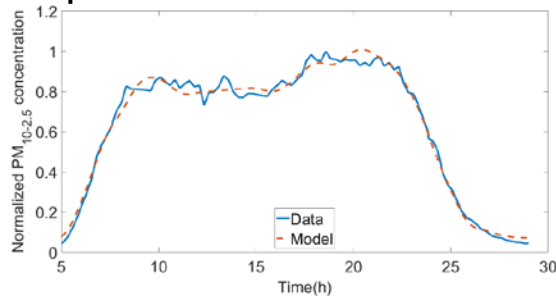


Fig. 6: Comparison of measured and simulated normalized $PM_{10-2.5}$ concentration on weekdays

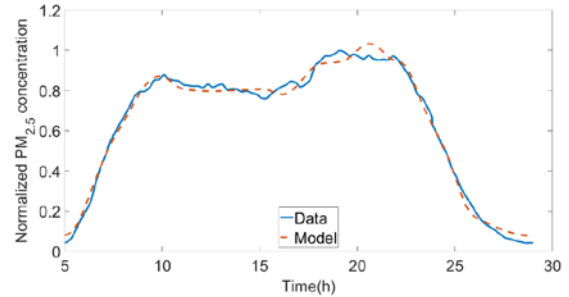


Fig. 7: Comparison of measured and simulated normalized $PM_{2.5}$ concentration on weekdays

The correlation for weekdays between PM measurements and model is good for the two class of particles with a determination coefficient of 0.990 for $PM_{10-2.5}$ and 0.991 for $PM_{2.5}$ (see figure 6 and 7). Identification is realized on median weekdays over a large period where boundary conditions probably varied (Outdoor PM concentrations and Airflows). Variations of mean natural airflow intensity is taken into account via v_n parameter but potential direction change of this natural ventilation from weather conditions can impact the results. Outdoor PM concentrations was set constant after data analysis as low variations were obtained after calculation of a mean day over the period.

Table 2: Parameters values after identification for $PM_{10-2.5}$ and for $PM_{2.5}$ class of PM

Term	Parameter	Unit	Value for $PM_{10-2.5}$	Value for $PM_{2.5}$
Emission	α_1 / α_2	$\mu\text{g.s.m}^{-3}$	0,478 / $3,30.10^{-4}$	0,418 / $3,17.10^{-4}$
Resuspension	ω_1 / ω_2	Dimensionless	$5,66.10^{-3}$ / $3,44.10^{-3}$	$5,09.10^{-3}$ / $4,34.10^{-3}$
Ventilation from train	v_t	Dimensionless	0,773	0,610
Natural ventilation	v_n	Dimensionless	0,150	0,120
Deposition	δ_1 / δ_2	s^{-1}	$2,18.10^{-3}$ / $2,29.10^{-3}$	$2,34.10^{-3}$ / $2,45.10^{-3}$

4.2. PM filtration analysis

Filtration solution installed in the station and composed of eight filtration devices was reproduced in the model. The filter media used in this example is assumed to have an efficiency ePM10 of 80% and ePM1 of 55% based on its data sheet. These efficiencies are defined in norm EN ISO 16890 and respectively evaluating efficiency for PM between 0.3 and $10\mu\text{m}$ and 0.3 and $1\mu\text{m}$. Based on the norm, ePM2.5 should be exceeding 65% and efficiency for $PM_{10-2.5}$ exceeding 95% (values used in the model).

Station is discretized by 25 volumes of 10m in the model in order to place precisely the filtration devices inside the station. The filtration sources only depend on aspiration flow and filter media efficiency here ($\epsilon=1$, no 3D CFD simulation results available yet).

Finally, simulations were launched and PM concentrations reduction can be seen on figure 8 for $PM_{10-2.5}$ and on figure 9 for $PM_{2.5}$ as red graph compared to the blue graph indicating the measured concentration at the station. Looking at the initial concentrations it is obvious that PM_{10} and $PM_{2.5}$ concentration levels show a similar shape of the graph, with it being stretched to larger values of concentration for PM_{10} . This is an expected trend which e.g. was also seen in the measurements performed by [14]. Nonetheless, the factor between both is different here and is expected not only to vary for different applications like outdoor and subway but also for different subway stations. The composition of the dust is special topic which is not within the focus of this article. The models used can be adapted for different dust sizes and give the flexibility to react to various real-life conditions. Evaluating the graphs showing the clean air again a similar shape is visible. This is also logical as the treatment of the reduction is linear dependent on the efficiency in the filtration term shown in equation (6). In consequence, the reduction graphs show the expected behaviour which can be interpreted as a successful implementation proof. To interpret the reduction ratios on global scale some things need to be considered.

The measured values give a mean of different situations being prominent during the measurements. This means wind directions can change, trains can enter, amount of people moving may vary, etc. All these things lead to the fact that the measured value is a statistical one, which shall not be interpreted as true for a single situation but as true for the overall picture and conditions. For sure, longer measurements will improve the statistical quality of the data.

The simulated efficiencies show around 32.4% reduction for PM_{10} and 35% for $PM_{2.5}$ which is closed to data obtained during the measurement campaign. Indeed, around respectively 34% and 36% were calculated from it. Considering the measurement accuracy of $\pm 0,75\%$ and the uncertainty given from boundary conditions this as a reasonable agreement.

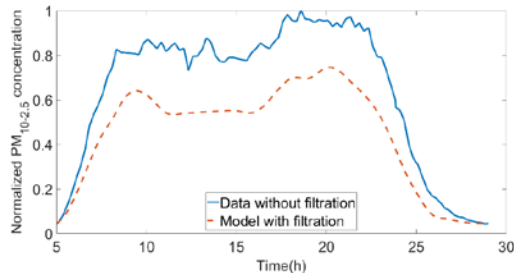


Fig. 8: Data 2020 without filtration versus simulated filtration solution of normalized $PM_{10-2.5}$ concentration on weekdays

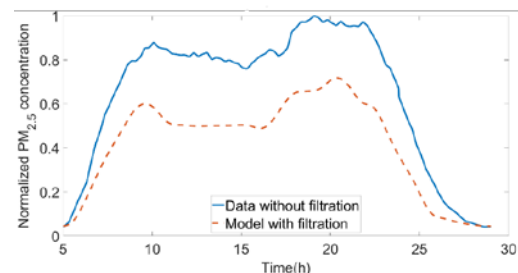


Fig. 9: Data 2020 without filtration versus simulated filtration solution of normalized $PM_{2.5}$ concentration on weekdays

Another empirical measurement that can be used to verify the simulation results is the mass captured by filtration devices. This is in general derived from the ambient air concentration, the runtime of the cleaning device, the volume flow and the efficiency. This data is extracted from the model for the two-size class of particles. $7g/device/day$ was measured in average during filtration period including all particle size up to $10\mu m$ and between 5.2 and $5.4g/device/day$ are obtained via simulation combining the two size classes under evaluation.

Finally, results obtained on this study case seem quite promising regarding median PM_{10} and $PM_{2.5}$ concentrations. Parameters identification allows for a good representation of these daily concentrations evolutions. Still, deposition rates have to be checked as they seem higher than what we can find in literature [15]. Filtration sources adding tested and compared with real measurement gives good results in terms of global efficiency and mass captured. These outputs are important criteria for the validation of the model. Indeed, poor parameters identifications would have given either a good global efficiency or a good mass captured but not both. Improvement of the results could be obtained after determination of the ϵ parameter linking 3D CFD results for filtration to 1D model. Concerning computation time, the test of a filtration configuration inside the station takes around a minute allowing comparison of a large number of configurations.

Next step which shall be investigated is dependency of the boundary conditions in a station to the model. Effects like concentration, ambient air flow speed and direction etc. may be of interest. Moreover, a study of different positions and operational points of the air cleaners will add up further knowledge and make it possible to optimize air cleaner layouts in subway stations. Overall, the question of the amount of measurement data to get statistically reliable statement for a station needs to be answered. Evidently, the transfer of the modelling approach to other stations and the comparison with measurement data is needed for final validation or calibration.

5. Conclusion

In this article, a novel method for the optimization of filtration solutions for subterranean train stations has been presented. This method is based on a model allowing an accurate particle concentration prediction for $PM_{10-2.5}$ and $PM_{2.5}$ over time and along the station platforms thanks to the discretization following train track direction. Indeed, daily PM concentrations dynamics linked to train activity are well described by the model. From this model and thanks to adaptable discretization length, filtration sources can be added and studied. 3D CFD can be used for filtration source calibration inside a discretized volume to precisely describe its global efficiency. This has been evaluated and compared with a real study case on the station presented in the paper. Global filtration efficiency inside the station and PM mass captured by filtration sources show good agreement with measurement.

Finally, this method will allow to optimize filtration solutions inside subterranean train station by defining the number and position of filtration source required for a given PM concentration target for example, or to test different filter media efficiency, optimize the aspiration airflow from filtration device over the day to limit the consumption or define the maintenance level thanks to the knowledge of PM captured mass per day.

Acknowledgements

The work in this article is done in a joint International Research Chair entitled “Filtration systems: fluid dynamics and energy consumption reduction” between MANN+HUMMEL and Ecole Centrale de Nantes. This research work is financially supported by the French Government and managed by the National Research Agency (ANR) with the Future Investments Program. The authors would like to express their gratitude to Anais Watbled from SNCF G&C DGIF for providing the concentration data and allowing their usage and Antonio Lozano for technical support during experimentation.

References

- [1] World Health Organization, ‘WHO global air quality guidelines: particulate matter (PM_{2.5} and PM₁₀), ozone, nitrogen dioxide, sulfur dioxide and carbon monoxide’, <https://www.who.int/publications-detail-redirect/9789240034228>, 2021.
- [2] M. Sarmadi, S. Rahimi, M. Rezaei, D. Sanaei, and M. Dianatinasab, ‘Air quality index variation before and after the onset of COVID-19 pandemic: a comprehensive study on 87 capital, industrial and polluted cities of the world’, *Environ. Sci. Eur.*, vol. 33, no. 1, p. 134, Dec. 2021.
- [3] C. B. P. D. Silva, P. Saldiva, L. F. Amato-Lourenço, Fernando Rodrigues-Silva, S. Miraglia, ‘Evaluation of the air quality benefits of the subway system in São Paulo, Brazil’, *J. Environ. Manage.*, vol. 101, pp. 191–196, Jun. 2012.
- [4] Agence Nationale de Sécurité Sanitaire Alimentation, Environnement, Travail, ‘Pollution chimique de l’air des enceintes de transport ferroviaires souterrains et risques sanitaires associés chez les travailleurs’, Sep. 2015.
- [5] S. Abbasi, A. Jansson, U. Sellgren, and U. Olofsson, ‘Particle Emissions From Rail Traffic: A Literature Review’, *Crit. Rev. Environ. Sci. Technol.*, vol. 43, no. 23, pp. 2511–2544, Jan. 2013.
- [6] Y. Cha, Y. Hedberg, N. Mei, and U. Olofsson, ‘Airborne Wear Particles Generated from Conductor Rail and Collector Shoe Contact: Influence of Sliding Velocity and Particle Size’, *Tribol. Lett.*, vol. 64, p. 40, Oct. 2016.
- [7] E. Walther, M. Bogdan, and R. Cohen, ‘Modelling of airborne particulate matter concentration in underground stations using a two size-class conservation model’, *Sci. Total Environ.*, vol. 607–608, pp. 1313–1319, Dec. 2017.
- [8] C. Henry, ‘Particle resuspension from complex surfaces: current knowledge and limitations’, *Cond-Mat Physicsphysics*, Feb. 2018.
- [9] V. Arrigoni, ‘Qualité de l’air dans les enceintes ferroviaires, une source : le freinage’, presented at the ATMOS’FAIR, Lyon, France, Oct. 2017.
- [10] B. Nasr, G. Ahmadi, A. R. Ferro, and S. Dhaniyala, ‘Overview of mechanistic particle resuspension models: comparison with compilation of experimental data’, *J. Adhes. Sci. Technol.*, vol. 33, no. 24, pp. 2631–2660, Dec. 2019.
- [11] A. C. K. Lai and W. W. Nazaroff, ‘Modeling indoor particle deposition from turbulent flow onto smooth surfaces’, *J. Aerosol Sci.*, vol. 31, no. 4, pp. 463–476, Apr. 2000.
- [12] J. J. Kim, T. Hann, and S. J. Lee, ‘Effect of flow and humidity on indoor deposition of particulate matter’, *Environ. Pollut.*, vol. 255, p. 113263, Dec. 2019.
- [13] *lsqcurvefit function*. Natick, Massachusetts: The MathWorks, Inc., 2019. [Online]. Available: <https://fr.mathworks.com/help/optim/ug/lsqcurvefit.html>
- [14] P. Bächler, T. K. Müller, T. Warth, T. Yildiz, and A. Dittler, ‘Impact of ambient air filters on PM concentration levels at an urban traffic hotspot (Stuttgart, Am Neckartor)’, *Atmospheric Pollut. Res.*, vol. 12, no. 6, p. 101059, Jun. 2021.
- [15] T. L. Thatcher, A. C. K. Lai, R. Moreno-Jackson, R. G. Sextro, and W. W. Nazaroff, ‘Effects of room furnishings and air speed on particle deposition rates indoors’, *Atmos. Environ.*, vol. 36, no. 11, pp. 1811–1819, Apr. 2002.